

Open Charm, Photon and Dilepton Production in an Increasingly Strongly Interacting Parton Plasma

S.M.H. Wong

Fachbereich Physik, Universität Wuppertal, D-42097 Wuppertal, Germany

We examine the effects of the new equilibration scenario of the increasingly strongly interacting parton plasma and of the non-equilibrium environment have on the production of open charm, photon and dilepton at LHC and at RHIC energies. We show that an out-of-equilibrium effect, not shown before, changes significantly the relative yield of the two main partonic contributions to photon production in the higher p_T range, and higher orders for electromagnetic emissions have increased significance in the new scenario especially at RHIC energies. We argue that the effects of the new scenario are not restricted just to the parton phase but will continue through to the later hadron gas phase with potentially positive implications for the detection of the quark-gluon plasma.

PACS number(s): 25.75.-q, 12.38.Mh, 13.87.Ce, 12.38.Bx

I. INTRODUCTION

Relativistic heavy ion collision experiments at the present AGS at Brookhaven and SPS at CERN and at the future colliders like RHIC and LHC aim to recreate deconfined matter or the quark-gluon plasma. In order to find out details in the collisions and to see whether the resulting highly compressed matter has made a return trip to the new phase through a phase transition, particle productions in the reactions provide the necessary means for the task. However, this is complicated by the fact that all particle signatures and probes can have their origins both from hadronic and partonic environment. This endeavor would have been much easier if productions from deconfined matter were significantly enhanced over the hadronic productions. Unfortunately, in practice, this is not always the case. In fact, one can only hope for excess in certain finite momentum range of the produced particles. The sizes of these windows depend on details such as the incoming energy/nucleon, parton distributions in the nucleus, etc.. It is vital therefore that production mechanisms behind both hadronic and partonic origins should be well understood and good quantitative control be obtained. In this paper, we consider three such particle productions from a partonic environment. We study two electromagnetic and a hadronic probe, namely photons and dileptons and open charm.

Electromagnetic probes are well known to be good probes because of their much weaker interactions and therefore they reflect the conditions of the production environment. These probes have been studied by many, for example [1–12], in both hadronic and partonic medium which could be in or out of equilibrium. Dilepton production could be, for instance, used to measure T_c [5]. Likewise, enhancement in soft dilepton production could be due to quark-gluon plasma formation [3,7] which would provide very good signals. However, background from bremsstrahlung off partons and pions [13] and also pion decays [5] and emission from hadronic scattering [14]

must also be considered. In the end, one has little choice but to rely on excess in a certain restricted momentum range of the produced electromagnetic radiation. Something similar can be said for photons. Their usefulness in helping to find the equation of state [15], reveal transverse expansion [16] or to see if a phase transition has occurred or not [8] have all been suggested. In this paper, we do not go into all these other possibilities of using electromagnetic emissions from the plasma, but we examine only the emission itself. We look for changes if any in the emission rates in the parton phase due to a change in the production environment brought about by a so-far-neglected new effect and also by the plasma being out-of-equilibrium. The cause and origin of the new effect will be discussed below.

Open charm is a hard hadronic probe of early dynamics [17–20] whose usefulness as a probe depends on the relative yield from the initial A+A collision and from the subsequent parton collisions, so any effects that could potentially shift the weight from one to the other production must be considered. That clearly includes parton distributions in a nucleus and hence nuclear shadowing [21] effect on the parton distributions and that of gluon in particular because of the initial gluon dominance. Recent DELPHI experiment at LEP has demonstrated, by measuring R_3^{bl} , the ratio of b-quark to lepton 3-jet fraction from Z decays, that the b-quark mass did run with scale [22–24]. The running mass $m_b(\mu)$ dropped to about 2.67 GeV at the Z mass scale. It seems logical therefore that one should also take into account the running of the charm quark mass when considering open charm production. How important is this effect for the charm mass will need to be determined. We will leave this as future investigation. In the following, we would not consider the initial production which has been done in the previous studies of open charm, but rather concentrate entirely in the production via the parton plasma.

Our main motivation in this investigation arises from a recently reported new equilibration scenario [25] which

starts right in the middle of that of the “hot glue” [26] and progressively gains importance in time. This is the scenario of the Increasingly Strongly Interacting Parton Plasma (ISIPP). The interactions get stronger and stronger with time in the plasma of quarks and gluons because the average parton energies drop due to longitudinal cooling and the “energy sharing” from parton creation. The resulting momentum transfers in the parton collisions are bound to decrease as a result. Therefore by choosing the most suitable renormalization scale in the strong coupling to reduce large logarithms from higher orders at all time during the time evolution of the plasma results naturally with a coupling that is increasing in strength with time. Note that there are two factors contributing to the decrease in momentum transfer, so one cannot hope to get rid of this increase in interaction strength in ISIPP just by shutting the plasma in a box to stop the expansion and hence longitudinal cooling. Parton chemical equilibration will make sure that ISIPP is here to stay even if there is no expansion. Thus a parton plasma is a rather unique kind of many-body system.

The effects of the increasing coupling on equilibration have been shown in [25] using the time evolution scheme developed in [27,28]. This new equilibration scenario means that the environment for particle production, at least, in the later parton plasma phase is no longer the same as has been considered so far. From what we have already mentioned at the beginning, the effects of this on particle production must be determined if one still wishes eventually to identify deconfined matter from the particle probes and signatures.

Another reason for our investigation in particle production is the environment itself. Because a non-equilibrium many-body system is non-trivial and is tied by its very nature to time evolution, most calculations restricted themselves to a simplified situation of a thermalized system. Thus any non-equilibrium effects on particle productions could not be revealed. We will show the presence of this in the case of photon production.

The effects of the ISIPP scenario on particle production can be roughly divided into two categories. They are the direct and indirect effects. Direct effect comes from those production mechanisms in which strong interactions play a part and therefore directly depends on α_s . Having said that, this effect is only operational if the production scale is roughly also the scale for equilibration. It is not operational if the scale of the production is always hard as in open charm production. Indirect effects, as can be guessed already, have not a direct dependent on the coupling. The influence of α_s comes via its effects on the equilibration or time evolution itself. More explicitly, they are the effects on the parton densities, duration of the parton phase etc.. The latter has an important role to play because the detectors measure what fall into them, when the particles were produced is of no consequence, so it is essential to integrate over the history of the collisions before drawing any conclusions on the relative yield from hadronic and deconfined

matter [4,8].

In the following sections, we will calculate and show the transverse momentum, p_T , or invariant mass, M , distribution for the three types of particle production already mentioned. We will compare the productions from a parton plasma time evolved with $\alpha_s = 0.3$ with those from the more consistent ISIPP for which the coupling is denoted by $\alpha_s = \alpha_s^v$ and its value as a function of time was extracted from the time evolution in [25]. In the original derivation of the time evolution equations, they were taken to be centered around the central region at $z = 0$ or $\eta = 0$ where the distributions were assumed to be more or less uniform. As a consequence, we do not perform the integration over spatial rapidity, or if one prefers, one can multiply by roughly a unit rapidity interval assuming uniform distribution around the central region. So our spacetime integration for particle production can be taken to be $\int d^4x = \pi R_A^2 \int \tau d\tau$. We will plot in all cases, p_T or M distribution at around zero spatial and particle rapidity. Since we are interested in the difference of the standard scenario and ISIPP, this should be sufficient to show the representative effects of the new time evolution on particle productions.

Our paper is organized as follows. We give the production rates and present results of the three types of particle production both from a parton plasma time evolved with a fixed coupling at essentially the standard value $\alpha_s = 0.3$ and from the ISIPP in Sec. II, III and IV. The results are discussed one by one. Then we move on to a discussion on higher orders, implications of ISIPP on particle production in general beyond the deconfined phase and other effects of ISIPP in relativistic heavy ion collisions.

II. OPEN CHARM PRODUCTION

Open charm production comes from gluon conversions, $gg \longleftrightarrow c\bar{c}$, and quark-antiquark annihilations $q\bar{q} \longleftrightarrow c\bar{c}$. Our results are calculated from

$$E \frac{d^7 N}{d^3 p d^4 x} = \frac{1}{2(2\pi)^3} \int \frac{d^3 \mathbf{k}_1}{(2\pi)^3 2\omega_1} \frac{d^3 \mathbf{k}_2}{(2\pi)^3 2\omega_2} \frac{d^3 \mathbf{p}'}{(2\pi)^3 2E'} \times (2\pi)^4 \delta^{(4)}(k_1 + k_2 - p' - p) \times \left\{ \frac{1}{2} \nu_g^2 f_g(k_1, \tau) f_g(k_2, \tau) |\mathcal{M}_{gg \rightarrow c\bar{c}}|^2 + \nu_q^2 f_q(k_1, \tau) f_q(k_2, \tau) |\mathcal{M}_{q\bar{q} \rightarrow c\bar{c}}|^2 \right\} \quad (1)$$

where $\nu_g = 2 \times 8 = 16$ and $\nu_q = 2 \times 3 \times n_f = 6n_f$ are the multiplicities of gluons and quarks, respectively. The distribution functions f_g and f_q are from our previous investigation on equilibration [25,28]. The matrix elements for $c\bar{c}$ production are [29]

$$|\mathcal{M}_{gg \rightarrow c\bar{c}}|^2 = \pi^2 \alpha_s^2 \left\{ \frac{12}{s^2} (m_c^2 - t)(m_c^2 - u) \right.$$

$$\begin{aligned}
& + \frac{8}{3} \left(\frac{m_c^2 - u}{m_c^2 - t} + \frac{m_c^2 - t}{m_c^2 - u} \right) \\
& - \frac{16m_c^2}{3} \left(\frac{m_c^2 + t}{(m_c^2 - t)^2} + \frac{m_c^2 + u}{(m_c^2 - u)^2} \right) \\
& - \frac{6}{s} (2m_c^2 - t - u) \\
& + \frac{6}{s} \frac{m_c^2 (t - u)^2}{(m_c^2 - t)(m_c^2 - u)} \\
& - \frac{2}{3} \frac{m_c^2 (s - 4m_c^2)}{(m_c^2 - t)(m_c^2 - u)} \} \quad (2)
\end{aligned}$$

for gluon conversion into charm-anticharm and

$$|\mathcal{M}_{q\bar{q} \rightarrow c\bar{c}}|^2 = \frac{64\pi^2 \alpha_s^2}{9s^2} \{ (m_c^2 - t)^2 + (m_c^2 - u)^2 + 2m_c^2 s \} \quad (3)$$

for quark-antiquark annihilation. We use an average like $\alpha_s = 0.3$ here in the production for both ISIPP and standard plasma because as we have already mentioned in Sec. I, open charm production is at a hard scale so the increasing coupling effect for equilibration only affects this through indirect effect of changes in parton densities and reduced production time. Since gluon conversion is the main contribution and the gluon density in ISIPP is reduced in general when compared to the standard plasma [25], combining this with reduced production time, there seems to be an unavoidable significant reduction in open charm yield.

In [19,20], it was shown that charm production from initial gluon conversion dominated pre-equilibrium production due to the suppression coming from spatial and momentum rapidity correlation of the produced minijet gluons, and thermal charm production was even smaller. Although initial production is dominant, both [19,20] rely on minijet gluon produced from HIJING [30–32] for the pre-equilibrium production. As remarked in [20], uncertainties in HIJING warrant some variations of the initial conditions at the time τ_{iso} in order to see what these uncertainties will lead. If a factor of 4 is given to the initial parton densities, pre-equilibrium production can be approximately equal or even larger than the initial production by gluon conversion. Thus one can make use of the sensitivity of open charm production to initial parton density as a means to probe the latter in high energy nuclear collisions. In view of the apparent reduction in yields pointed out above due to the effects of the coupling, the use of charm as a probe becomes more doubtful. This is in fact not the case. The reason will be given below after we have shown our results of the actual production and compared the different scenarios.

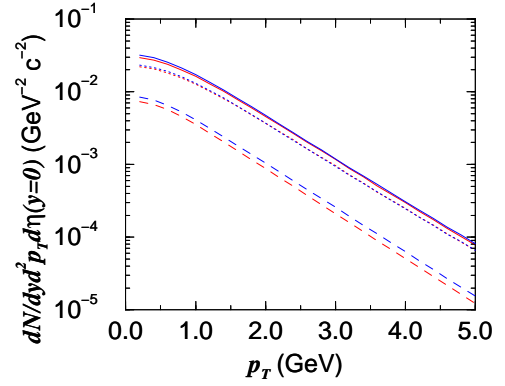


FIG. 1. Comparison of charm production in a parton plasma produced at LHC energies, which is time evolved with an evolving coupling α_s^v , with the one time evolved with a fixed $\alpha_s = 0.3$. For the production itself, we used $\alpha_s = 0.3$ in all cases because this is a hard process. Dotted and dashed lines are for gluon conversion and quark-antiquark annihilation contribution, respectively. Solid lines are the sum total. Lines from ISIPP tend to lie slightly below the corresponding lines from the fixed $\alpha_s = 0.3$ evolved plasma. It is more clearly so for annihilation contribution.

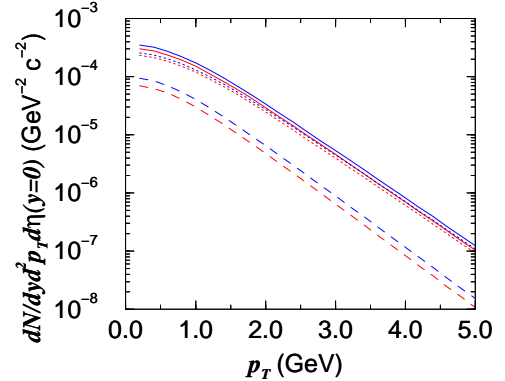


FIG. 2. Same as in Fig. 1 but for a parton plasma produced at RHIC energies.

In Fig. 1 and Fig. 2, we plotted the charm yield at LHC and at RHIC as a function of p_T at central rapidity. We have not used K-factor in obtaining our plots because the production ratio of the two scenarios was our main concern. The dotted and dashed lines are for contributions from gluon conversion and quark-antiquark annihilation, respectively. The full lines are for the total contributions. The set of three lines for ISIPP lies just below the corresponding lines for $\alpha_s = 0.3$ case. As can be seen from Fig. 1 at LHC and Fig. 2 at RHIC, both gluon conversion and quark-antiquark annihilation contribution from ISIPP are slightly reduced when compared with those of the standard parton plasma. The reduction of the latter contribution is more substantial because although the fermion densities in ISIPP are higher due to more significant conversion of gluons into light fermion pairs, this contribution is more spread out in time, whereas

the bulk of the gluon conversion contribution tends to be from early times, this we have checked, and so is less affected by the reduction in the production time. For the same reason, the effect of lowered gluon density, due to the near saturation and the conversion into fermion pairs which eventually take toll on the number of gluons present, essentially does not manifest on the plot.

The total charm yield at LHC is then about the same in the two cases and at RHIC, there is a slight reduction. So although there is no direct effect to help the production, due to the different scales of the production itself and that of equilibration, and there is a reduction in the production time which hints at a potential reduction in open charm yield, when all factors were considered, the yield is essentially unchanged in the parton plasma in the new scenario. The usefulness of charm as a probe of initial parton densities concluded in [19,20] is therefore retained. It is interesting, however, to see how the spread of the contributions to charm production during the history of the plasma can avoid certain effects of the coupling on the final yields.

Having said that a definite conclusion on how good charm as a probe is cannot be completely settled at present due to uncertainties in the nuclear shadowing effect on the nuclear gluon distribution used to calculate the charm production from initial gluon conversion. But there are some recent advances on predicting shadowing effect, see [33]. Also, as already mentioned in the Sec. I, the importance of the running mass effect must be checked. Clearly all enhancement and suppression factors in the production during the two different stages must be identified. Here we checked that in the new scenario, there is no significant modification to the p_T -distribution of production from the parton plasma.

III. PHOTON PRODUCTION

Photon production comes from Compton scattering $gg \rightarrow q\gamma$ or $\bar{q}g \rightarrow \bar{q}\gamma$ and quark-antiquark annihilation $q\bar{q} \rightarrow g\gamma$. The production rate is given by

$$\begin{aligned}
E \frac{d^7 N}{d^3 p d^4 x} &= \frac{1}{2(2\pi)^3} \int \frac{d^3 \mathbf{k}_1}{(2\pi)^3 2\omega_1} \frac{d^3 \mathbf{k}_2}{(2\pi)^3 2\omega_2} \frac{d^3 \mathbf{k}_3}{(2\pi)^3 2\omega_3} \\
&\times (2\pi)^4 \delta^{(4)}(k_1 + k_2 - k_3 - p) \\
&\times \left\{ 2f_g(k_1, \tau) f_q(k_2, \tau) (1 - f_q(k_3, \tau)) \right. \\
&\quad \times |\mathcal{M}_{gq \rightarrow q\gamma}|^2 \\
&\quad + f_{\bar{q}}(k_1, \tau) f_{\bar{q}}(k_2, \tau) (1 + f_g(k_3, \tau)) \\
&\quad \left. \times |\mathcal{M}_{q\bar{q} \rightarrow g\gamma}|^2 \right\}. \tag{4}
\end{aligned}$$

A factor of two has been included for the two possibilities of Compton scattering off quark and antiquark. The matrix elements, which include colour and spin as well as

infrared screened by the time-dependent medium quark mass [27,28],

$$m_q^2(\tau) = 4\pi\alpha_s \left(\frac{N_c^2 - 1}{2N_c} \right) \int \frac{d^3 \mathbf{k}}{(2\pi)^3 k} (f_g(k, \tau) + f_q(k, \tau)), \tag{5}$$

are

$$|\mathcal{M}_{gq \rightarrow q\gamma}|^2 = - \sum_q e_q^2 2^9 \pi^2 \alpha_s \left\{ \frac{s}{t - m_q^2} + \frac{t}{s + m_q^2} \right\}, \tag{6}$$

for emission through Compton scattering and

$$|\mathcal{M}_{q\bar{q} \rightarrow g\gamma}|^2 = \sum_q e_q^2 2^9 \pi^2 \alpha_s \left\{ \frac{u}{t - m_q^2} + \frac{t}{u - m_q^2} \right\}, \tag{7}$$

for that through quark-antiquark annihilation. In the modulus squared of the matrix elements, we set the renormalized coupling $\alpha_s = \alpha_s^v$ for the ISIPP scenario because the scale of the production processes is on the average, unlike the hard process of open charm production, roughly the same as the scale for parton collisions in equilibration. The same also applies to dilepton production, which we will consider up to next-to-leading order in the renormalized coupling in Sect. IV later on.

The p_T distribution is plotted in Fig. 3 and Fig. 4 for photon production at LHC and at RHIC, respectively. The dotted lines are for production from Compton scattering and dashed lines from quark-antiquark annihilation. The total are the solid lines. We have already mentioned the indirect effects of the coupling on the plasma in the previous section. In photon production, there is a single power of α_s in the modulus squared amplitude in Eq. (6) and Eq. (7), which constitutes a direct effect on the production. However, in spite of the fact that ISIPP evolution caused a drop in the gluon density and a reduction in the parton phase duration in comparison to those of the evolution of the conventional plasma, the increase in quark and antiquark densities plus the progressively increasing interaction strength compensate for the negative effects in the total sum. The curves in the two scenarios lie almost on top of each other as a result.

At this point, we would like to point out an out-of-equilibrium effect, which as far as we are aware, has never been shown before. It is certainly of interest from a theoretical point of view. We will discuss its practical significance at the end of this section once we have shown and explained its origin.

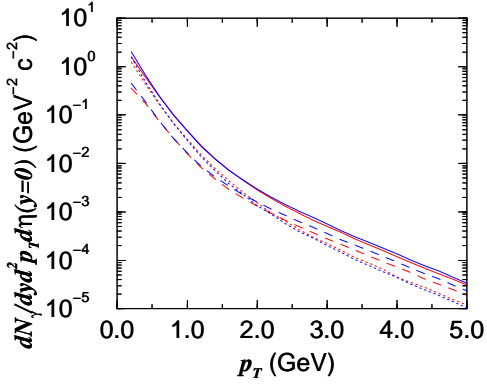


FIG. 3. Photon production from the parton plasma at LHC. The solid lines are the total sum of the emission from Compton scattering (dotted) and quark-antiquark annihilation (dashed). At large p_T , quark-antiquark annihilation is the dominant contribution because of the fact that quarks and gluons are not in equilibrium with respect to each other and are therefore at different effective temperatures and of quantum statistical effect to a lesser extent. This contribution from the standard parton plasma is slightly above that from ISIPP at large p_T .

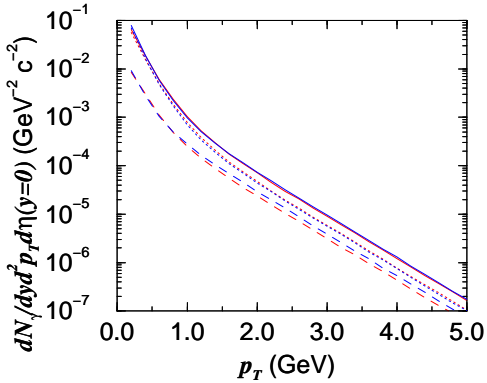


FIG. 4. Same as Fig. 3 but at RHIC. In this case, however, emissions from Compton scattering remain above those from quark-antiquark annihilation up to $p_T = 5.0$ GeV because of the much lower quark to gluon density ratio at RHIC. The point where the emission from the latter begin to dominate over the former is at higher p_T beyond 5.0 GeV.

In Fig. 3, it is seen that emission from Compton scattering at LHC does not dominate over that from quark-antiquark annihilation throughout the whole p_T range unlike that shown in [16]. This is because in [16], the distribution for the final state emitted parton has been dropped and hence quantum statistical effect, such as stimulated emission, was excluded. The more important reason, however, is the parton plasma in [16] was taken to be in kinetic equilibrium, an out-of-equilibrium effect coming in through the particle distributions of the incoming partons could not therefore manifest and, as we will explain in the next paragraphs, is the cause of the dominance of annihilation over Compton scattering con-

tribution at higher p_T at LHC.

In [25,28], we showed that quarks and gluons in the plasma were not in equilibrium with respect to each other and that they could be considered to be at different effective temperatures. The more rapid cooling of gluons due to the combined effect of gluon multiplication and conversion into quark-antiquark meant that gluons were at a lower temperature effectively most of the time than that of quarks and antiquarks. Apart from the more obvious Pauli blocking, stimulated emission and the different matrix elements, the difference between Compton scattering and annihilation contribution comes from the distributions $f_g(k_1, \tau)$ and $f_q(k_1, \tau)$ in Eq. (4). It is this last difference which is responsible for the effect of the dominance of photon emission from quark-antiquark annihilation over Compton scattering at larger p_T .

As can be seen in Fig. 3, the effect is stronger at higher p_T so we can try to explain it by concentrating in this p_T range. Although the plasma is not in equilibrium, nevertheless, we can simplify the argument by taking f_g and f_q as essentially of equilibrium form but at different temperatures. Furthermore, large p_T photon emission requires high energy incoming partons so $f_g(k_1)$ and $f_q(k_1)$ can be taken to be of Boltzmann form $l_g \exp(-k_1^0/T_g)$ and $l_q \exp(-k_1^0/T_q)$. So if the values of the temperatures and fugacities are such that $(l_q/l_g) \exp\{k_1^0(1/T_g - 1/T_q)\} > 1$, the annihilation contribution will acquire an enhancement over Compton scattering contribution. This relative enhancement requires some time to build up as the effective temperatures have to cool sufficiently so that the exponential can more than compensate for the ratio $l_q/l_g < 1$. At LHC, the larger ratio of n_q/n_g and the longer duration of the parton phase allow the manifestation of this enhancement at about $p_T = 1.6$ GeV already. At RHIC, the lower ratio of n_q/n_g and the shorter duration do not permit this at $p_T < 5.0$ GeV but the effect is there as one moves to higher and higher p_T photon. As can be seen in Fig. 4, the annihilation contribution is approaching that from Compton scattering as p_T increases. At low p_T , the effect is still there because both low and high energy incoming partons contribute but the former are the dominant contribution in this case, so high p_T photons are needed to select out harder incoming partons to see this effect. Note that this is not a density effect since the ratio of the quark to gluon density $n_q/n_g < 1$ always both at LHC and at RHIC, but is that of different components of the plasma at different effective temperatures. The density or fugacity ratio only determines at which point during the time evolution this effect comes in. So, by using emission from Compton scattering as a bench mark, with the out-of-equilibrium and quantum statistical effect, photon emission from the quark-gluon plasma can have a better chance to compete with direct photon and photon fragmented off minijets at large p_T [34] and hence enlarges the window for observing photon emission from deconfined matter.

IV. DILEPTON PRODUCTION

The leading dilepton production rate is, for massless quarks and leptons, and adopted to our time-evolving environment, given by [1,2]

$$\frac{d^8 N_{\mu^+\mu^-}^{(1)}}{d^4 x d^4 q} = \int \frac{d^3 \mathbf{k}_1}{(2\pi)^3} \frac{d^3 \mathbf{k}_2}{(2\pi)^3} f_q(k_1, \tau) f_q(k_2, \tau) \times \delta^{(4)}(k_1 + k_2 - q) v_{rel} \sigma_{q\bar{q} \rightarrow \mu^+\mu^-}(M) \quad (8)$$

where $q^2 = M^2$ is the invariant mass squared of the dilepton pair*, $\sigma_{q\bar{q} \rightarrow \mu^+\mu^-}(M) = 12 \sum_q e_q^2 \tilde{\sigma}(M)$ is the cross-section for quark-antiquark annihilation into a dilepton pair. The relative velocity $v_{rel} = M^2/2\omega_1\omega_2$ is that of the quark-antiquark pair and $\tilde{\sigma}(M) = 4\pi\alpha^2/3M^2$ is the cross-section of $e^+e^- \rightarrow \mu^+\mu^-$.

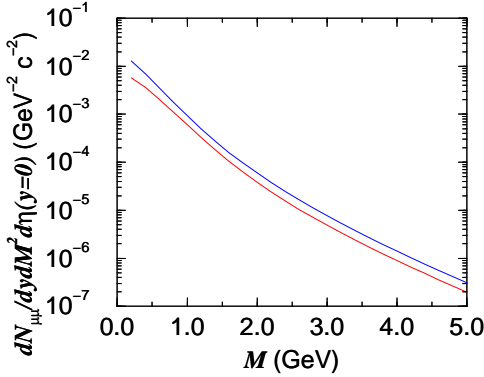


FIG. 5. Comparison of dilepton emission from an ordinary parton plasma (upper solid line) with ISIPP (lower solid line) at LHC. Even though the fermion densities are enhanced in ISIPP, the shortening of the duration of the plasma in the parton phase is the more important of the two effects. So the emission from ISIPP is reduced.

For both standard plasma and ISIPP, the invariant mass distributions for dilepton production are shown in Fig. 5 and Fig. 6. Both at LHC in Fig. 5, and at RHIC in Fig. 6, the dilepton yields from ISIPP are below those from the standard parton plasma. In the absence of direct effect, the enhanced quark-antiquark densities are not sufficient to compensate for the shortened duration of the ISIPP. The production in ISIPP are down by an approximate factor of 1.6 at LHC and 1.9 at RHIC on the average. The size of the window for observing dilepton production from the parton plasma will therefore, unfortunately, be reduced at least from the production during the time interval we considered. Of course, to get the complete picture, one has to take into account production before our initial time τ_0 and from the mixed phase in the case of a first order phase transition.

*We write $\mu^+\mu^-$ here to represent dilepton pair.

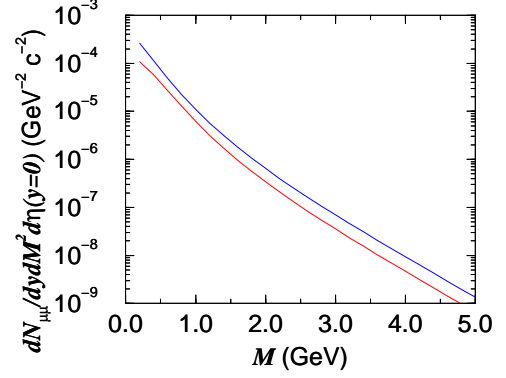


FIG. 6. Same as in Fig. 5 but at RHIC. Again, emission from ISIPP (lower) is below that from a standard parton plasma (upper).

Since the leading order contribution is only subjected to indirect effect of the coupling, we also work out the next-to-leading order contributions, from non-interference graphs only, to get a glimpse of higher orders. We have to mention that the following is not a consistent calculation of higher order contributions because the time evolution of the plasma was done with interactions at leading order [25,28] and so the following results should be viewed as an explorative study. The non-interference Feynman graphs at the next-to-leading order are similar to those of the photon production except the photon is now off-shell and timelike. Again as in real photon production, we have Compton and annihilation contributions. The production rate is

$$\begin{aligned} \frac{d^4 N_{\mu^+\mu^-}^{(\alpha_s)}}{d^4 x} &= \int \frac{d^3 \mathbf{k}_1}{(2\pi)^3 2\omega_1} \frac{d^3 \mathbf{k}_2}{(2\pi)^3 2\omega_2} \frac{d^3 \mathbf{k}_3}{(2\pi)^3 2\omega_3} \frac{d^3 \mathbf{l}_1}{(2\pi)^3 2l_1^0} \\ &\times \frac{d^3 \mathbf{l}_2}{(2\pi)^3 2l_2^0} (2\pi)^4 \delta^{(4)}(k_1 + k_2 - k_3 - l_1 - l_2) \\ &\times \left\{ 2f_g(k_1, \tau) f_q(k_2, \tau) (1 - f_q(k_3, \tau)) \right. \\ &\quad \times |\mathcal{M}_{gq \rightarrow q\mu^+\mu^-}|^2 \\ &\quad + f_q(k_1, \tau) f_q(k_2, \tau) (1 + f_g(k_3, \tau)) \\ &\quad \left. \times |\mathcal{M}_{q\bar{q} \rightarrow g\mu^+\mu^-}|^2 \right\}. \quad (9) \end{aligned}$$

This can be rewritten as

$$\begin{aligned} \frac{d^8 N_{\mu^+\mu^-}^{(\alpha_s)}}{d^4 x d^4 q} &= \int \frac{d^3 \mathbf{k}_1}{(2\pi)^3 2\omega_1} \frac{d^3 \mathbf{k}_2}{(2\pi)^3 2\omega_2} \frac{d^3 \mathbf{k}_3}{(2\pi)^3 2\omega_3} \\ &\times \delta^{(4)}(k_1 + k_2 - k_3 - q) \frac{2q^0 \Gamma_{\gamma^* \rightarrow \mu^+\mu^-}(M)}{M^4} \\ &\times \left\{ 2f_g(k_1, \tau) f_q(k_2, \tau) (1 - f_q(k_3, \tau)) \right. \\ &\quad \times |\mathcal{M}_{gq \rightarrow q\gamma^*}|^2 \\ &\quad + f_q(k_1, \tau) f_q(k_2, \tau) (1 + f_g(k_3, \tau)) \\ &\quad \left. \times |\mathcal{M}_{q\bar{q} \rightarrow g\gamma^*}|^2 \right\} \quad (10) \end{aligned}$$

in terms of the decay width of a timelike virtual photon into a dilepton pair, which is given by

$$\Gamma_{\gamma^* \rightarrow \mu^+ \mu^-}(M) = \frac{1}{2q^0} \int \frac{d^3 \mathbf{l}_1}{(2\pi)^3 2l_1^0} \frac{d^3 \mathbf{l}_2}{(2\pi)^3 2l_2^0} \times (2\pi)^4 \delta^{(4)}(q - l_1 - l_2) |\mathcal{M}_{\gamma^* \rightarrow \mu^+ \mu^-}|^2. \quad (11)$$

The sum over final states and averaged over initial state matrix element squared is $|\mathcal{M}_{\gamma^* \rightarrow \mu^+ \mu^-}|^2 = 2^4 \pi \alpha M^2 / 3$ and so the decay width is $\Gamma_{\gamma^* \rightarrow \mu^+ \mu^-}(M) = \alpha M^2 / 3q^0$.

The other matrix element squared for virtual photon production [35] via Compton scattering, including again colour, spin and infrared screening, is

$$|\mathcal{M}_{gq \rightarrow g\gamma^*}|^2 = \sum_q e_q^2 2^9 \pi^2 \alpha \alpha_s \left\{ -\frac{t}{s+m_q^2} - \frac{s}{t-m_q^2} + 2M^2 \left(\frac{1}{t-m_q^2} + \frac{1}{s+m_q^2} - \frac{M^2}{(s+m_q^2)(t-m_q^2)} \right) \right\} \quad (12)$$

and that from annihilation is

$$|\mathcal{M}_{q\bar{q} \rightarrow g\gamma^*}|^2 = \sum_q e_q^2 2^9 \pi^2 \alpha \alpha_s \left\{ \frac{t}{u-m_q^2} + \frac{u}{t-m_q^2} - 2M^2 \left(\frac{1}{t-m_q^2} + \frac{1}{u-m_q^2} - \frac{M^2}{(u-m_q^2)(t-m_q^2)} \right) \right\}. \quad (13)$$

There is an additional infrared divergence hidden in $f_g(k_3)$ in the annihilation contribution when very soft gluon is emitted with the photon, we cut this off by requiring $k_3 \geq m_g$, the gluon mass in the medium. This problem is not present in real photon production because there k_3 can only reach zero when $s = 0$ when the modulus squared of the matrix element vanishes. This latter in the present virtual photon case does not vanish. We use $m_g^2 = \frac{1}{3}m_D^2$, the relation between the gluon mass and the Debye screening mass in equilibrium, and m_D^2 is calculated similarly from the time-dependent quark and gluon distribution [27,28].

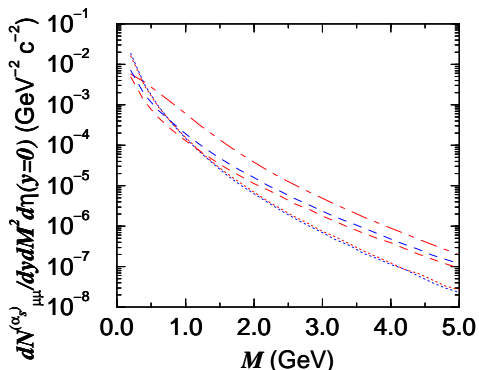


FIG. 7. Dilepton emission at next-to-leading order at LHC from ISIPP and from the standard parton plasma. Timelike virtual photon emissions from quark-antiquark annihilation (dashed) dominate over those from Compton scattering (dotted) at higher values and in fact most values of M because of the combined effect of interference and quantum statistics. The two sets of curves from ISIPP and from the standard plasma lie almost on top of each other with the annihilation contribution from the standard plasma slightly higher due to the smaller cutoff of the gluon mass in the medium, and so are, similar to real photon production at leading order, essentially the same for both scenarios. Emission at leading order from ISIPP (dot-dashed) is plotted again for comparison.

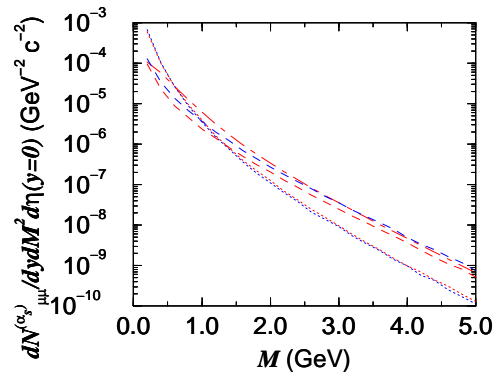


FIG. 8. Same as in Fig. 7 but at RHIC. In this case, the annihilation contribution (lower dashed) is much closer to the leading order contribution (dot-dashed) from ISIPP at larger M .

The next-to-leading order results are plotted in Fig. 7 at LHC and in Fig. 8 at RHIC. Like photon production at leading order, negative and positive direct and indirect effects largely cancel out each other so that the invariant mass distribution from ISIPP and from the standard parton plasma are very similar. The small decrease of the more dominant annihilation contribution from ISIPP, the lower of the two dashed curves in each figure, is due to the gluon mass cutoff used, which is larger in ISIPP. In the present case, annihilation contribution dominates at large M because of the interference effect in the matrix elements for timelike virtual photon emission. This is the more important, the larger the value of M . This reduces Compton scattering but increases annihilation contribution. This is however not a medium effect. What is the result of medium effect and has to do with the increasing interaction strength is the difference of the production rate between the leading and next-to-leading order. If one examines, for example Fig. 6 and Fig. 8, the leading order and the next-to-leading order are closer to each other in ISIPP than in the standard parton plasma, so higher orders are more comparable to the leading order especially at RHIC energies. Therefore in general in ISIPP, higher orders are more important for dilepton production in heavy ion collisions as a result of the increasing coupling effect.

V. SUMMARY AND OUTLOOK

We have examined the effects of the coupling and out-of-equilibrium environment had on three types of particle production in the new ISIPP scenario. We found that although at first sight there seemed to be an unavoidable reduction in the open charm yield, the concentration of the contribution from gluon in the early times prevented a significant diminution in the yield. As such, the usefulness of open charm as a probe of early parton densities is not affected. For photon production, a non-equilibrium effect not shown previously which came about as a result of quark-antiquark and gluon existing as a mixed fluid with different effective temperatures and with different cooling rates, brought the quark and antiquark annihilation contribution to photon production, in the higher p_T region, to above that from Compton scattering. Whereas in a thermally equilibrated plasma, Compton scattering would dominate in the same region. For dilepton production, something similar happened but this time, it was due to quantum interference effect. The more interesting medium effect we found by an explorative study into higher order contributions in this case was that ISIPP rendered the leading and next-to-leading order contributions to be comparable with each other especially at RHIC. Thus higher orders seem to have greater significance in ISIPP than in the standard parton plasma. This could be viewed as a possible representative result of how higher orders could affect non-hard type processes such as the electromagnetic productions considered here. But before we can study particle production more closely, higher orders have first to be included in the time evolution of the system.

In this work, we restricted our considerations on the effects of ISIPP on particle productions to the deconfined phase. Apparently, there is a lack of enhancement that one would hope for. However, bearing in mind that the ratio of hadronic and partonic signals is more crucial for the search for the quark-gluon plasma, a reduction in hadronic signals would be just as good. It must be mentioned that the effects of ISIPP extend well beyond the parton phase because of the effects on the entropy during the equilibration of the parton plasma. As shown in [25], entropy would be reduced more significantly in the parton plasma, the larger is the coupling. So entropy reduction in ISIPP would reduce the duration of the mixed phase if there is a first order phase transition. The signals from this phase will be affected in a certain way. One can imagine the increasing coupling effects of the direct and indirect type will continue to be effective for signals of partonic origin. But for signals of hadronic origin, they will only be subjected to indirect effects. These, when applied to the hadronic part of the mixed phase and the subsequent hadron phase, apart from the reduced duration of the former already mentioned, in view of the entropy reduction, will lead to a lowered final hadron multiplicity and hence hadron gas density. The latter

would mean weaker hadronic signals. Since direct effect tends to be stronger than indirect ones, if higher orders are taken into account, then signals of partonic origin, but not those of hard processes, will at least remain the same if not actually be enhanced, but those of hadronic origin will be suppressed. Therefore the effects of the interaction strength of the parton plasma could shift the balance of certain signals, for example electromagnetic ones, emitted from relativistic heavy ion collisions experiments in favour of those of partonic origin and thus the search for the quark-gluon plasma would be made easier than before.

While we were finishing this paper, we received two papers [36,37], in which the authors also pointed out quite rightly and discussed the importance of running both in the strong coupling and in the quark mass in thermal flavour production. It seems that one should also consider this in the initial as well as in the early minijet gluon conversion stage especially for charm for the purpose of comparison. As we discussed here, the running coupling effects are more general and wide ranging and should be taken into account not only for flavour production in the quark-gluon plasma.

ACKNOWLEDGEMENTS

The author would like to thank K. Redlich for useful discussion on photon production.

-
- [1] L.D. McLerran and T. Toimela, Phys. Rev. D **31**, 545 (1985).
 - [2] K. Kajantie, J. Kapusta, L. McLerran and A. Mekjian, Phys. Rev. D **34**, 2746 (1986).
 - [3] E. Braaten, R.D. Pisarski and C.P. Yuan, Phys. Rev. Lett. **64**, 2242 (1990).
 - [4] J. Kapusta, P. Lichard and D. Seibert, Phys. Rev. D **44**, 2774 (1991).
 - [5] H.A. Weldon, Phys. Rev. Lett. **66**, 293 (1991).
 - [6] R. Baier, H. Nakkagawa, A. Niégawa and K. Redlich, Z. Phys. C **53**, 433 (1992).
 - [7] S.M.H. Wong, Z. Phys. C **53**, 465 (1992).
 - [8] S. Chakrabarty, J. Alam, D.K. Srivastava and B. Sinha, Phys. Rev. D **46**, 3802 (1992).
 - [9] K. Geiger and J.I. Kapusta, Phys. Rev. Lett. **70**, 1920 (1993).
 - [10] E.V. Shuryak and L. Xiong, Phys. Rev. Lett. **70**, 2241 (1993).
 - [11] C.T. Traxler, H. Vija and M.H. Thoma, Phys. Lett. B **346**, 329 (1995).
 - [12] C.T. Traxler and M.H. Thoma, Phys. Rev. C **53**, 1348 (1996).
 - [13] D. Pal, P.K. Roy, S. Sarkar, D.K. Srivastava, and B. Sinha, Phys. Rev. C **55**, 1467 (1997).

- [14] R. Baier, M. Dirks and K. Redlich, Phys. Rev. D **55**, 4344 (1997).
- [15] J. Cleymans, R. Redlich and D.K. Srivastava, preprint nucl-th/9702004.
- [16] B. Müller, M.G. Mustafa, D.K. Srivastava, Phys. Rev. C **56**, 1064 (1997).
- [17] B. Müller and X.N. Wang, Phys. Rev. C **51**, 3326 (1995).
- [18] K. Geiger, Phys. Rev. D **48**, 4129 (1993).
- [19] Z. Lin and M. Gyulassy, Phys. Rev. C **51**, 2177 (1995).
- [20] P. Lévai, B. Müller and X.N. Wang, Phys. Rev. C **51**, 3326 (1995).
- [21] K.J. Eskola, Nucl. Phys. B **400**, 240 (1993).
- [22] W. Bernreuther, A. Brandenburg and P. Uwer, Phys. Rev. Lett. **79**, 189 (1997).
- [23] S. Martí i García, J. Fuster and S. Cabrera, talk presented at QCD'97, Montpellier, France, July 97, hep-ex/9708030.
- [24] M. Bilenky, G. Rodrigo and A. Santamaria, Phys. Rev. Lett. **79**, 193 (1997).
- [25] S.M.H. Wong, Phys. Rev. C **56**, 1075 (1997).
- [26] E.V. Shuryak, Phys. Rev. Lett. **68**, 3270 (1992).
- [27] S.M.H. Wong, Nucl. Phys. A **607**, 442 (1996).
- [28] S.M.H. Wong, Phys. Rev. C **54**, 2588 (1996).
- [29] B.L. Combridge, Nucl. Phys. B **151**, 429 (1979).
- [30] M. Gyulassy and X.N. Wang, Phys. Rev. D **44**, 3501 (1991).
- [31] M. Gyulassy, M. Plümer, M. Thoma and X.N. Wang, Nucl. Phys. A **538**, 37c (1992).
- [32] M. Gyulassy and X.N. Wang, Nucl. Phys. A **544**, 559c (1992).
- [33] Z. Huang, H.J. Lu and I. Sarcevic, preprint AZPH-TH/97-07, hep-ph/9705250.
- [34] S. Gupta, Phys. Lett. B **248**, 453 (1990).
- [35] R.D. Field, *Applications of Perturbative QCD*, Frontiers in Physics Vol. 77 (Addison-Wesley, Redwood City, CA, 1986).
- [36] J. Letessier, J. Rafelski and A. Tounsi, Phys. Lett. B **389**, 586 (1996).
- [37] J. Letessier, J. Rafelski and A. Tounsi, in *Proceedings of ICHEP'96*, edited by Z. Ajduk and K. Wroblewski. (World Scientific, Singapore, 1997), p. 971.

FIGURE CAPTIONS

Fig. 1 Comparison of charm production in a parton plasma produced at LHC energies, which is time evolved with an evolving coupling α_s^v , with the one time evolved with a fixed $\alpha_s = 0.3$. For the production itself, we used $\alpha_s = 0.3$ in all cases because this is a hard process. Dotted and dashed lines are for gluon conversion and quark-antiquark annihilation contribution respectively. Solid lines are the sum total. Lines from ISIPP tend to lie slightly below the corresponding lines from the fixed $\alpha_s = 0.3$ evolved plasma. It is more clearly so for annihilation contribution.

Fig. 2 Same as in Fig. 1 but for a parton plasma produced at RHIC energies.

Fig. 3 Photon production from the parton plasma at LHC. The solid lines are the total sum of the emission from Compton scattering (dotted) and quark-antiquark annihilation (dashed). At large p_T , quark-antiquark annihilation is the dominant contribution because of the fact that quarks and gluons are not in equilibrium with respect to each other and are therefore at different effective temperatures and of quantum statistical effect to a lesser extent. This contribution from the standard parton plasma is slightly above that from ISIPP at large p_T .

Fig. 4 Same as Fig. 3 but at RHIC. In this case, however, emissions from Compton scattering remain above those from quark-antiquark annihilation up to $p_T = 5.0$ GeV because of the much lower quark to gluon density ratio at RHIC. The point where the emission from the latter begin to dominate over the former is at higher p_T beyond 5.0 GeV.

Fig. 5 Comparison of dilepton emission from an ordinary parton plasma (upper solid line) with ISIPP (lower solid line) at LHC. Even though the fermion densities are enhanced in ISIPP, the shortening of the duration of the plasma in the parton phase is the more important of the two effects. So the emission from ISIPP is reduced.

Fig. 6 Same as in Fig. 5 but at RHIC. Again, emission from ISIPP (lower) is below that from a standard parton plasma (upper).

Fig. 7 Dilepton emission at next-to-leading order at LHC from ISIPP and from the standard parton plasma. Timelike virtual photon emissions from quark-antiquark annihilation (dashed) dominate over those from Compton scattering (dotted) at higher values and in fact most values of M because of the combined effect of interference and quantum statistics. The two sets of curves from ISIPP and from

the standard plasma lie almost on top of each other with the annihilation contribution from the standard plasma slightly higher due to the smaller cut-off of the gluon mass in the medium, and so are, similar to real photon production at leading order, essentially the same for both scenarios. Emission at leading order from ISIPP (dot-dashed) is plotted again for comparison.

Fig. 8 Same as in Fig. 7 but at RHIC. In this case, the annihilation contribution (lower dashed) is much closer to the leading order contribution (dot-dashed) from ISIPP at larger M .